FIRST EVALUATIONS OF NON LINEAR ELASTIC EFFECTS IN LGT CRYSTALS BY COMBINED PULSE-ECHO AND RESONATOR METHODS

C. HUBERT, T. ABERLENC, M. GAUTHIER, M. FISCHER and A. POLIAN

Laboratoire de Physique des Milieux Condensés, CNRS UMR 7602, Université Pierre et Marie CURIE, 4, Place Jussieu, B77, 75252 PARIS CEDEX 05, FRANCE

J.J. BOY, E. BIGLER, R. BOURQUIN and B. DULMET,

LCEP-ENSMM, 26 Avenue de l'Observatoire, 25030 Besancon cedex - FRANCE

ABSTRACT

Non linear elastic effects in LGT crystals have been measured by two different methods : pulse-echo wave velocity measurements under hydrostatic pressure and diametrical compression of thickness-shear resonators. The same samples of LGT crystals have been used to fabricate both kinds of samples so a direct comparison of non-linear elastic effects between both experiments are meaningful.

1. INTRODUCTION

In this paper, we present the pressure dependence of the elastic moduli of one important and promising member of the langasite family: $La_3Ta_{0,5}Ga_{5,5}O_{14}$ (Langatate: LGT).

From the same crystal, thickness shear resonators have been fabricated and tested under diametrical compression. Two kinds of resonators with .39 and . 54 mm thickness have been used and frequency shifts under diametrical compression are coherent with a figure for the force-frequency coefficient of 5.4 10-15 m.s/N, a factor 4 smaller than for AT-cut quartz.

2. EXPERIMENTAL PROCEDURE AND RESULTS

2.1 Choice of measurement directions

The crystal of Langatate has a trigonal structure (class 32) like quartz : it has six independent Second Order Elastic Constants (SOEC), so, at least, six experiments are required to determine completely the second order elastic constants tensor

The samples orientations were chosen to prevent the measurements which contain piezoelectric contributions, so all stiffened mode have been eliminated.

2.2 samples orientations and dimensions

The Cartesian coordinate system was chosen so that the Z axis coincides with the optic triad axis, X axis is parallel to one of the twofold symmetry axis, and Y axis completes the right-handed coordinate system. Two types of samples were studied : the first one are small parallelepipeds oriented along the Z axis cut according to the previously defined convention and the seconds are cut at 45 degrees from Y axis.

The samples used are large parallelepipeds with various dimensions ranging from 4.97 to 6.93 mm. Their density value is r=6,126 g.cm ^{3}.

2.3 Pulse echo overlap method

The measurement of the round travel time of an ultrasonic pulse in the sample is obtained by a pulse-echo overlap method. This method consits in the superposition of different echoes, obtained after several reflection on the rear face of the sample.

To achieve a very good pulse overlap, it is necessary to have a very short pulse in time to be distinguished, but which contains a sufficient number of arc in order to have the most accurate measurement (Fig. 1).

Moreover, an analysis software based upon the signal correlation have been developed in the laboratory in order to improve the results accuracy.

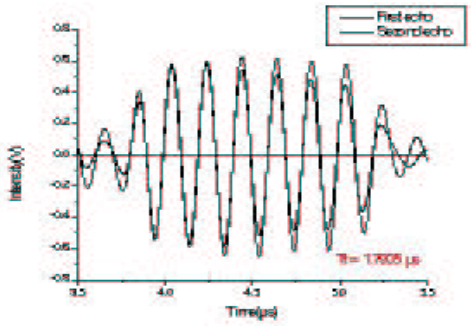

Fig1Example of an pulse overlapping

2.4 Experimental devices

2.4.1 Transducers

Two types of transducers have been used :

Piezoelectric ceramics with longitudinal and shear polarizations which have the same resonance frequency at 7 MHz for ambient pressure measurements.

Oriented plates of lithium niobate, with the same resonance frequency of 10 MHz for longitudinal and shear mode, for hydrostatic pressure measurements.

2.4.1 Pressure device

The hydrostatic pressure up to 0,2 GPa has been obtained by using a piston-cylinder apparatus using a low viscosity oil as a pressure transmitting medium.

2.5 Results and discussion

2.5.1 Ambient pressure

In table 1, the ultrasonic determination of the six second order elastic constants is shown.

The results of reference 2, 3 and 4 are given for comparison. As a general rule, they are in good agreement with ours , except for the reference 4. The results for this reference is obtained by a surface acoustic wave method which is well known to be less accurate and so not very appropriate for the SOEC ψ tensor determination. Moreover, an other LGS SOEC set is given to show that results for LGT and LGS are of the same order of magnitude.

Table 2 :Comparison of the elastic moduli of LGT (in GPa)

	C_{11}	C_{12}	C_{13}	C_{14}	C_{33}	C_{44}	C_{66}
This work	190.9 ±1.5	111.4 ±4.5	92.4 ±9.1	13.5 ±0.9	265.9 ±0.7	51.2 ±0.1	39.8 ±2.9
[Ref. 2]	190.9	107.9	73.9	13.7	263.2	51.2	41.5
[Ref. 3]	188.9	108.1	100.8	13.9	264.4	51.2	40.4
[Ref. 4]	202	120	125	13.3	288	49.7	40.7
LGS *	189.3	105	95.3	13.5	260.5	50.4	40.7

*LGS=$La_3Ga_5 SiO_{14}$ [Ref.2]

2.5.2 Hydrostatic pressure

Hydrostatic pressure measurements give the pressure dependence of the round travel time in the sample, for a pressure up to 0.2 GPa. A rapid analysis of these measurements show that the round travel time has a linear behavior with pressure

For each values of pressure, we can determine elastic moduli by the measurement of the round travel time. Since the pressure range is small(0.2 GPa), we can consider that the linear and volume compressibilities are constants to calculate the length and the density of the sample at each pressure.

Thanks to the relations between elastic moduli and SOEC, we can evaluate the linear behavior of SOEC for this pressure range:

$$C_{IJ}(P)=C_{IJ}(P=0)+(\partial C_{ij}/\partial P)P \qquad (1)$$

Table 2 : Pressure derivatives of SOEC

	$\frac{\partial C_{11}}{\partial P}$	$\frac{\partial C_{12}}{\partial P}$	$\frac{\partial C_{13}}{\partial P}$	$\frac{\partial C_{14}}{\partial P}$	$\frac{\partial C_{33}}{\partial P}$	$\frac{\partial C_{44}}{\partial P}$
LGT	+19.70	+7.60	1.70	+0.06	+15.70	+2.12

All the pressure derivatives are positive, except for C_{13}.

2.5.3 Determination of TOEC combination

The following formula links SOEC pressure derivatives to some third order elastic constants (TOEC) combinations [5] :

$$\partial C_{ij}/\partial P=-\chi_a(C_{Ui}+C_{Uj})-\chi_c C_{Uk} \qquad (2)$$

where: χ_a (=2.7.10^{-3}) and χ_c (=1.8.10^{-3}) are respectively the linear compressibilities in GPa^{-1}, along the a and c axis.

So we can deduce these TOEC combinations :

$$\partial C_{11}/\partial P=-\chi_a(C_{111}+C_{112})-\chi_c C_{113} \qquad (2.1)$$

$$\partial C_{12}/\partial P=-\chi_a(C_{112}+C_{122})-\chi_c C_{123} \qquad (2.2)$$

$$\partial C_{13}/\partial P=-\chi_a(C_{113}+C_{123})-\chi_c C_{133} \qquad (2.3)$$

$$\partial C_{14}/\partial P=-\chi_a(C_{114}+C_{124})-\chi_c C_{134} \qquad (2.4)$$

$$\partial C_{33}/\partial P=-2\chi_a C_{133}-\chi_c C_{333} \qquad (2.5)$$

$$\partial C_{44}/\partial P=-\chi_a(C_{144}+C_{155})-\chi_c C_{344} \qquad (2.6)$$

There are only 6 different combinations relations with SOEC pressure derivatives to determine 14 TOEC. So, it is necessary to use other methods measurements to determine the whole set of TOEC.

3. FORCE FREQUENCY EFFECT

The above mentioned resonators have been tested in a force frequency apparatus (Fig. 1b) built on purpose and previously used [5]. A vertical load, namely 1 Kg, is repeatedly applied on the edge, along a diameter of the resonator. For singly rotated cuts, the direction of the force, with respect to the crystallographic X-axis, is defined on Fig. 1 by the azimuthal angle psi.

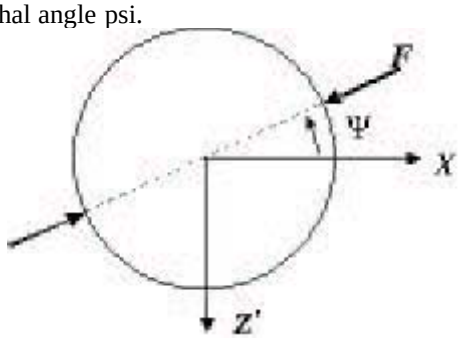

Fig. 2 : Definition of the psi angle

A typical order of magnitude of this effect is +/-20 to 50 Hz at 10 MHz for 1 Kg load.

Plots of the force frequency effect versus y angle are represented on Fig. 3a (thickness 0.394 mm) and Fig. 3b (thickness 0.542 mm for 11MHz 5th overtone) for the LGT resonators. The overall shape of the curve is sinusoidal, as is well known for quartz [12] where is defined an intrinsic coefficient which it is called Kf :

(3)

non-linear elastic coefficients and of static strain.

where *D* is the diameter, *t* the thickness, *F* the force expressed in N and N_0 being the velocity constant. The expression of the relative frequency shift depends

on the effective elastic coefficient expressed in term of linear and non-linear elastic coefficients and of static strain.

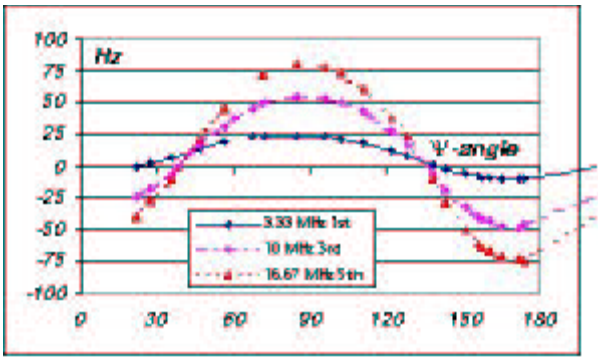

Fig. 3a : LGT resonators (0.394 mm thick) : Df versus psi angle

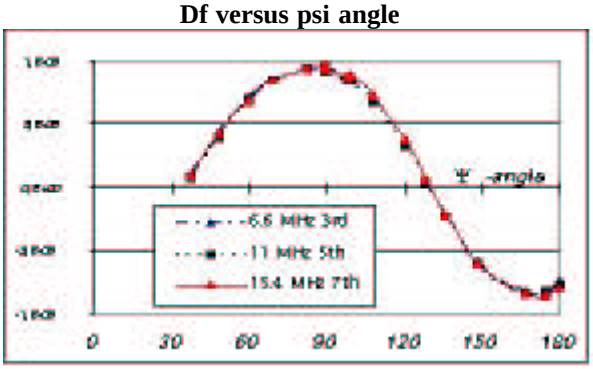

Fig. 3b : LGT resonators (0.542 mm thick) : Df/f versus psi angle

The experimental data presented in the figures 3a and 3b can be compared with those obtained with quartz resonators. For an AT-cut quartz resonator, the maximum value of the force frequency effect is obtained with the azimuthal angle Y =0 and, in this X-direction, the relative frequency shift due to 1 Kg load applied on a 11MHz 5th overtone is : 3.7 x 10-5. A similar resonator in Langatate exhibits a maximum relative frequency shift close to 10-5 for Y = 90° (Fig. 3b). And the maximum relative frequency shift for a 1 Kg load applied on the edge of a SC-cut 10MHz 3rd overtone is close to 3 x 10-5.

In the next figure (Fig. 4), we present the force-frequency effect of the Y-cut 10MHz 3rd overtone built in Langasite. The theoretical model, previously developed for quartz [10], has been used to compare the theoretical prediction with experimental data. The model is based on previously published material constants by Sakharov et al. [6] and Alexandrov et al. [13]. In the case of quartz, the agreement between calculated and measured values for Kf is good. But, we observe that, in our case, for LGS crystal, only general shape and anisotropy dependence is correctly modeled. As can be seen on this Fig. 4, the existence of- ñeutral points" of zero force sensitivity is found. However, a major discrepancy is found for the magnitude of this effect.

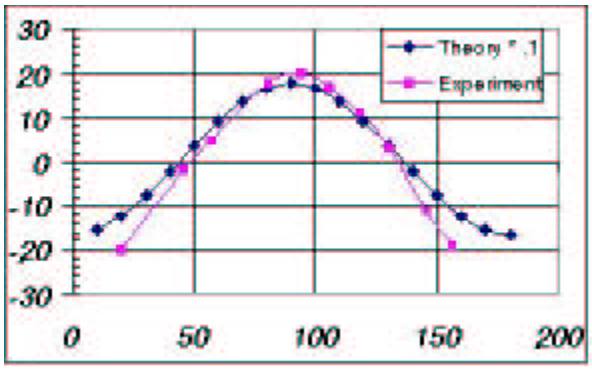

Fig. 4 : LGS resonator - comparison between theory and experiment (Df versus azimuthal angle)

The situation is really puzzling because the apparatus and the model were both extensively used for quartz with good results [5]. The only change in the computing model was entering material constants. It is for this reason that we present the following figure in order to show the influence of the accuracy of constants on Kf behavior (Fig. 5).

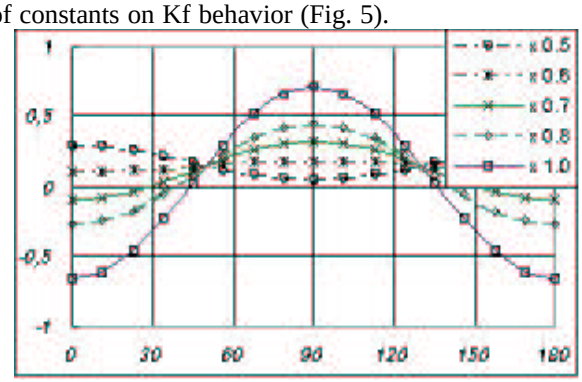

Fig. 5 : Influence of the predicted values of the third order elastic coefficients on the force-frequency effect on Langasite resonator (normalized values)

Indeed, if we apply a scaling factor to the set of the third order elastic coefficients used in the Kf calculation, we can observe significant changes in the force-frequency effect showing that the effect of the third order coefficients can be balanced by the effect of the second onFinally, we can summarize our observations as indicated in the following table :

Table 4 : maximum Kf values for Y-cuts on LGS and LGT crystals and various cuts on quartz crystal

	y (for max)	Kf value x 10-15 m. s/N
Y-cut LGS	90	0.8
Y-cut LGT	90	5.4
AT-cut quartz	0	22
SC-cut quartz	43	12

4. CONCLUSIONS

Results for the SOEC determination at ambient pressure are presented. This results are compared with references and seems to be in good agreement.

The evolution of the SOEC with pressure up to 0.2 GPa is measured. But we need also other methods to determine the complete set of TOEC independently, like uniaxial stress or harmonic generation methods.

Plano-convex LGS and LGT resonators have been fabricated, their electrical parameters measured and the force frequency experimentally studied. Even if the second order temperature coefficient of Y-cut is higher than AT or SC-cuts quartz, this LGS / LGT Y-cut exhibits interesting properties in terms of stress sensitivity.

The theoretically predicted magnitude of Kf is about half the value of Kf for AT-cut quartz, the experimental results being even smaller by at least a factor 3. The anisotropy dependence of the effect is very symmetrical, somewhat similar to the SC cut of quartz : the interesting perspective is that resonators built from LGS-cuts in the vicinity of the Y-cut will exhibit, like SC-cut quartz resonators, a reduced sensitivity to radial stresses.

As a consequence, the bridges of BVA type resonators have to be oriented in the directions of zero sensitivities, as indicated on figures 3 and 4.

ACKNOWLEDGEMENTS

We want to thank Dr Stepanov from VNIISIMS and Dr R.C. Smythe from Piezo Technology Inc. for providing samples of Langasite and Langatate.

REFERENCES

[1] D. ROYER, E. DIEULESAINT, "Ondes élastiques dans les solides," tome1, MASSON (1996)

[2] B. V. MILL, Y. V. PISAREVSKY, "Langasite-type materials : from discovery to present state," 2000 IEEE/EIA International Frequency Control Symposium and Exhibition (2000).

[3] E. CHILLA, C.M. FLANNERY and H. J. FROHLICH, "Elastic properties of langasite-type crystals determined by bulk and surface acoustic wave," Journal of Applied Physics Vol. 90, number 12 (2001).

[4] N. ONOZATO, M. ADACHI and T. KARAKI, Japanese Journal of Applied Physics Vol. 39, pp 3028, Part 2 (2000).

[5] R. N. THURSTON, H.J. McSKIMIN, and P. ANDREATCH, Journal of Applied Physics Vol. 37, pp 267, Number 1 (1965).

[6]. S. SAKHAROV et al. IEEE Inter. Freq. Cont. Symp., pp. 647, 652 (1995)

[7]. BAUMHAUER, H.F. TIERSTEN J. Acoust. Soc. Am. N°54, pp. 1017, 1034 (1973)

[8]. H. F. TIERSTEN J. Acoust. Soc. Am. Vol. 64, N°3, pp. 832, 837 (1978)

[9]. D.S. STEVENS, H.F. TIERSTEN J. Acoust. Soc. Am. VOL. 79, N°6, pp. 1811, 1826 (1986).

[10]. R. BOURQUIN, B. DULMET Proc. 41st, A. F.C.S. pp. 289, 294 (1987).

[11]. J. DETAINT et al. Proc. of 9th E.F.T.F., pp. 289, 296 (1995).

[12]. J. M. RATAJSKI Proc. of 20th A.F.C.S., pp. 39, 46 (1966).

[13]. K.S. ALEXANDROV et al. IEEE Ultrasonics Symp., pp. 409, 412 (1995).